**DOI**: 10.13208/j.electrochem.161104 **Artical ID**:1006-3471(2017)06-0708-10
**Cite this**: *J. Electrochem.* **2017**, *23*(6): 708-717 **Http**://electrochem.xmu.edu.cn

# Electroactivities of $Pd/Fe_3O_4$-C Catalysts for Electro-Oxidation of Methanol, Ethanol and Propanol

ZOU Tao[1], YI Qing-feng[1,2*], ZHANG Yuan-yuan[1], LIU Xiao-ping[1],
XU Guo-rong[1], NIE Hui-dong[1], ZHOU Xiu-lin[1]
(1. *School of Chemistry and Chemical Engineering, Hunan University of Science and Technology, Xiangtan* 411201, *China*; 2. *Key Laboratory of Theoretical Organic Chemistry and Functional Molecule, Ministry of Education, Xiangtan* 411201, *Hunan, China*)

**Abstract**: Development of palladium (Pd) catalysts with high electroactivity for alcohol oxidation is significant for alcohol fuel cells. In this work, Pd nanoparticles were formed by sodium borohydride ($NaBH_4$) reduction method and subsequently deposited on the surface of carbon supported ferriferrous oxide ($Fe_3O_4$/C) composite to obtain the $Pd/Fe_3O_4$-C catalysts with different $Fe_3O_4$ loadings. Their transmission electron microscopic (TEM) images show that the Pd nanoparticles were uniformly dispersed on the $Fe_3O_4$/C. Electroactivities of the prepared $Pd/Fe_3O_4$-C catalysts towards oxidation of C1-C3 alcohols (methanol, ethanol, *n*-propanol and iso-propanol) in alkaline media were investigated by cyclic voltammetry (CV), chronoamperometry and electrochemical impedance spectroscopy. Among the prepared catalysts ($Pd/Fe_3O_4$(2%)-C, $Pd/Fe_3O_4$(5%)-C, $Pd/Fe_3O_4$(10%)-C and Pd/C), the $Pd/Fe_3O_4$(5%)-C catalyst presented the highest electro-oxidation current density for oxidation of C1-C3 alcohols. According to the CV data, the anodic peak current densities for oxidation of methanol, ethanol, *n*-propanol and iso-propanol on the $Pd/Fe_3O_4$(5%)-C catalyst were over 1.7, 1.4, 1.7 and 1.3 times larger than that on the Pd/C catalyst, respectively. Furthermore, the charge transfer resistance of ethanol oxidation on the $Pd/Fe_3O_4$(5%)-C catalyst was much lower than that on the Pd/C catalyst. For all of the prepared catalysts, the decreases in electro-oxidation current density of the tested C1-C3 alcohols followed the order of *n*-propanol > ethanol > methanol > iso-propanol. In addition, the presence of $Fe_3O_4$ nanoparticles in the carbon powder improved the electrochemical stability of the Pd nanoparticles.

**Key words:** Pd catalyst; $Fe_3O_4$; alcohol oxidation; electrocatalyst
**CLC Number**: O646 **Document Code**: A

Direct alcohol fuel cells (DAFCs) are of significant interest from both energy and environmental considerations. Anode reaction in DAFCs is electro-oxidation of alcohols, which has been extensively investigated in recent decades[1-7]. It has been recognized that platinum (Pt) and Pt-based catalysts are the best electro-catalysts for alcohol oxidation. Unfortunately, practical application of the Pt-based catalysts is seriously limited because of the high cost and rare resources of Pt. In addition, poisoning effect of Pt surface, caused by the intermediate product like carbon monoxide (CO) produced during the alcohol electro-oxidation, also results in the decline of the electroactivity. Ferriferrous oxide ($Fe_3O_4$) has been reported to present unique catalytic and environmental friendly properties[8], and has been therefore used to improve the electroactivity of Pt-based catalysts. Huang et al has prepared a novel yolk/shell $Fe_3O_4$-polydopaminee-graphene-Pt ($Fe_3O_4$@PDA/RGO/Pt) nanocomposite that exhibited lower over-potential, higher electrocatalytic activity and notably stability for methanol oxidation than Pt/graphene[9]. Hong has syn-

Received: 2016-11-04, Revised: 2017-03-17 *Corresponding author, (86-731)58290045, E-mail: yqfyy2001@hnust.edu.cn
This work was financially supported by the National Natural Science Foundation of China (No.21376070) and the Hunan Provincial Natural Science Foundation of China (No.14JJ2096).

thesized $Fe_3O_4$-supported Au and Pt nanoparticles ($Pt/Au/Fe_3O_4$) using the conventional sodium borohydride ($NaBH_4$) reduction method, and found that the $Pt/Au/Fe_3O_4$ catalyst showed a significant enhancement on electroactivity for methanol oxidation compared to the Pt/Au/C catalyst[10]. Furthermore, the addition of nano $Fe_3O_4$ in activated carbon air cathode was beneficial to boosting the charge transfer of oxygen reduction reaction accompanying with the enhancement of power performance in microbial fuel cell[11]. Another ideal alternative to Pt is palladium (Pd) due to the much lower cost of Pd than Pt. The Pd and Pd-based catalysts showed even higher electroactivity for alcohol oxidation in alkaline media than Pt despite no obvious electroactivity of Pd for alcohol oxidation in acidic media. Electroactivity of the Pd catalyst could be further improved by alloying Pd with other metals or forming of Pd-based composites[12-16]. Electroactivity of the Pd catalyst for alcohol oxidation was promoted by nanocrystalline oxides including $CeO_2$, $Co_3O_4$, $Mn_3O_4$, and NiO[17-18]. Shen and coworkers reported that Pd-NiO/C catalyst showed a higher over-potential for the oxidation of CO than Pd/C and Pt-NiO/C catalysts[18]. This would be explained in terms of two possible mechanisms: 1) adsorption of ethanol on the surface of Pd-NiO/C is in the ascendant compared to that of CO, and 2) no CO is formed for ethanol oxidation on the Pd-NiO/C.

In this work, the carbon-supported $Fe_3O_4$ nanoparticles ($Fe_3O_4$-C) with different $Fe_3O_4$ mass loadings were firstly prepared according to the reference [19], and then the $Pd/Fe_3O_4$-C catalysts with different mass ratios of Pd to $Fe_3O_4$ were prepared by using $PdCl_2$ as the Pd precursor and $Fe_3O_4$-C as the substrate. Their electroactivities for electro-oxidation of alcohols (methanol, ethanol, *n*-propanol and iso-propanol) in alkaline media were investigated by voltammetric techniques and electrochemical impedance spectroscopy.

## 1 Experimental

All chemicals used in this work were of analytical grade and used as received without further purification. $Fe_3O_4$ nanoparticles and carbon power were purchased from Sinopharm Group Chemical Regent Co. Ltd. Water was deionized water subjected to the double distillation. The catalysts were synthesized by the conventional $NaBH_4$ reduction method. Firstly, the carbon-supported $Fe_3O_4$ nanoparticles ($Fe_3O_4$-C) were prepared according to the following steps as described previously[19]. $x$ mg of $Fe_3O_4$ nanoparticles and 100 mg of carbon powder were mixed with 20 mL of ethyl acetate, and the mixture was subjected to sonication treatment for 1 h at room temperature. The formed suspension was then distilled in vacuo at 40 ℃ to remove the solvent. The black powder was $Fe_3O_4$-C composite. Three $Fe_3O_4$-C composites, named as $Fe_3O_4$(2%)-C, $Fe_3O_4$(5%)-C and $Fe_3O_4$(10%)-C, corresponding to the $Fe_3O_4$ mass percentages of 2%, 5% and 10%, respectively, were obtained when the $x$ values ($Fe_3O_4$ mass) were 2.1, 5.3 and 11.1 mg, respectively. The $Fe_3O_4$-C supported Pd nanoparticles were synthesized by using the as-prepared $Fe_3O_4$-C as the substrate and $PdCl_2$ as the metal precursor. The $Fe_3O_4$-C and $PdCl_2$ were ultra-sonically mixed in ethylene glycol to form a uniform suspension. Then, excess 20% $NaBH_4$ solution in ethylene glycol was added to the suspension drop by drop under stirring, and the obtained suspension was kept stirring for 4 h. Afterward, it was filtered and then washed by abundant amounts of water to remove the impurities dissolved in the suspension. The black residue was vacuum-dried at 40 ℃ for 24 h to obtain the $Pd/Fe_3O_4$-C catalyst. Three $Pd/Fe_3O_4$-C catalysts, labelled as $Pd/Fe_3O_4$(2%)-C, $Pd/Fe_3O_4$(5%)-C and $Pd/Fe_3O_4$(10%)-C, were prepared by using $Fe_3O_4$(2%)-C, $Fe_3O_4$(5%)-C and $Fe_3O_4$(10%)-C as the supports, respectively. For comparison, the Pd/C was prepared by using the same method as the $Pd/Fe_3O_4$-C catalysts except the carbon powder instead of $Fe_3O_4$-C being used. TEM images of the prepared catalysts were recorded using a transmission electron microscope system (TEM, Philips, the Netherlands).

Electrochemical measurements were carried out in a conventional three-electrode glass cell with an AutoLab PGSTAT30/FRA electrochemical instrument (the Netherlands). The working electrode was a

thin film of ink on a glassy carbon disk electrode (GC, 0.071 $cm^2$). The ink was made by ultrasonically mixing 5 mg of the catalyst sample with 0.95 mL of ethanol and 50 μL of 5 wt% Nafion solution. Then, 12 μL of the suspension ink was dropped onto the GC electrode and left to dry in air at room temperature. A Pt foil and Ag/AgCl in saturated KCl solution acted as the counter and reference electrodes, respectively. All potentials were referred to Ag/AgCl electrode. Prior to experiments, pure nitrogen gas (99.99%) was bubbled through the solution for at least 15 min to remove the dissolved oxygen in the solution. Before electrochemical measurements, working electrodes were cleaned by repeatedly cycling scans in a range of -1.0 to 0.6 V in 1 mol·$L^{-1}$ NaOH solution until reproducible CV profiles were obtained. All experiments were performed at room temperature (25 ± 2) ℃.

## 2 Results and Discussion

Fig. 1 shows the TEM images of the prepared catalysts. Inset in Fig. 1A indicates that the size of $Fe_3O_4$(10)-C particles was ca. 33 nm. The larger grey particles with sizes of 35 ~ 40 nm were carbon support. The smaller dark dots in Fig. 1 A dispersed on the carbon support, were the Pd nanoparticles with an average particle size of ca. 4.9 nm. Some particles formed aggregates as indicated in the circles (Fig. 1A). For the Pd particles deposited on $Fe_3O_4$-C support, their Pd particle sizes were ca. 13 nm for Pd/$Fe_3O_4$(2%)-C (Fig. 1B), ca. 5 nm for Pd/$Fe_3O_4$(5%)-C (Fig. 1C) and 7 nm for Pd/$Fe_3O_4$(10%)-C (Fig. 1D). Although the Pd particles supported on $Fe_3O_4$-C were larger than those on carbon, no obvious aggregate was found from Pd/$Fe_3O_4$(2%)-C, Pd/$Fe_3O_4$(5%)-C and Pd/$Fe_3O_4$(10%)-C catalysts.

XRD patterns of the catalysts are shown in Fig. 2. There were four diffraction peaks at 2$\theta$ values of ca. 39.9°, 46.5°, 67.9° and 81.9° that are indexed to the (111), (200), (220) and (311) planes of Pd face-centered cubic (fcc) crystal structure, respectively. The weak diffraction peaks appearing at 2$\theta$ values of ca. 35.5° and 62.7° could be attributed to the (311) and (440) planes of $Fe_3O_4$. Other diffraction peaks belonged to $Fe_3O_4$ at 30.2°, 37.2°, 43.2°, 53.5° and 57.2° were not presented, which may be associated with the lower $Fe_3O_4$ content or the enshrouded $Fe_3O_4$.

Fig. 3 shows the cyclic voltammetric (CV) data on the prepared catalysts in 1 mol·$L^{-1}$ NaOH solution. These catalysts presented characteristic CV profiles of polycrystalline Pd electrode. All catalysts exhibited a cathodic peak r at ca. -0.35 to -0.36 V, which is ascribed to the reduction of Pd oxides produced during the forward potential scan. This cathodic peak current density reduced following the order: Pd/$Fe_3O_4$-(5%)-C > Pd/$Fe_3O_4$(2%)-C > Pd/$Fe_3O_4$(10%)-C > Pd/C. In addition, the real surface areas involved to Pd active sites ($S_{active\ Pd}$) for these Pd-based catalysts can be reckoned according to the coulombs consumed for the

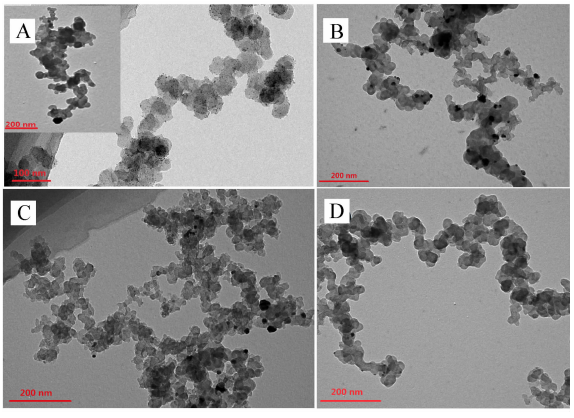


Fig. 1 TEM images of the Pd/C (A), Pd/$Fe_3O_4$(2%)-C (B), Pd/$Fe_3O_4$(5%)-C (C) and Pd/$Fe_3O_4$(10%)-C (D) catalysts. Inset in Fig. 1A is $Fe_3O_4$-C TEM image.

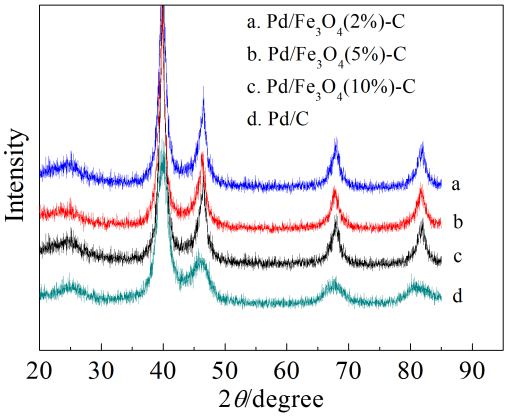


Fig. 2 XRD patterns of the prepared catalysts Pd/$Fe_3O_4$(2%)-C (a), Pd/$Fe_3O_4$(5%)-C (b) Pd/$Fe_3O_4$(10%)-C (c) and Pd/C (d)

reduction of Pd oxides (cathodic peak r) formed during the forward scan on the smooth polycrystalline Pd electrode (CV not shown). The evaluated Sactive Pd values of the Pd/$Fe_3O_4$(2%)-C, Pd/$Fe_3O_4$(5%)-C, Pd/$Fe_3O_4$(10%)-C and Pd/C catalysts were 4.70, 5.88, 2.40 and 2.83 $cm^2$, respectively, which are significantly larger than their geometrical area of 0.071 $cm^2$. The largest Pd active surface area was achieved with the Pd/$Fe_3O_4$(5%)-C catalyst among the four prepared catalysts. It is suggested that the addition of an appropriate amount of $Fe_3O_4$ to carbon is more propitious to the dispersion of Pd nanoparticles.

Cyclic voltammograms of the prepared catalysts

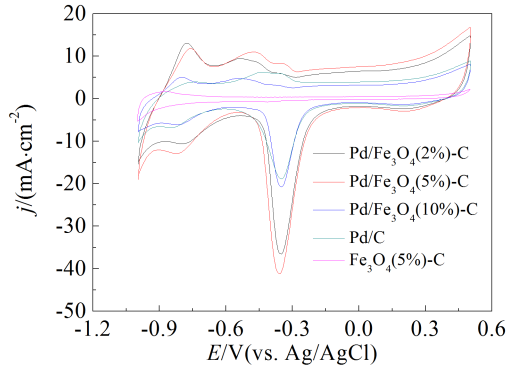


Fig. 3 Cyclic voltammograms of different catalysts in 1 mol·$L^{-1}$ NaOH solutions at a scan rate of 50 mV·$s^{-1}$

in NaOH solutions containing different alcohols are presented in Fig. 4. It is clearly seen from Fig. 4 that $Fe_3O_4$(5%)/C showed no electrocatalytic activity for the oxidation of the alcohols tested in this work. As for methanol oxidation in Fig. 4A, all catalysts containing $Fe_3O_4$ displayed a similar CV profile to Pd/C, characterized by a large anodic peak on the positive-going scan ($r_p$) and a relatively small one on the negative-going scan ($r_n$). Compared to the Pd/C catalyst, Pd/$Fe_3O_4$(2%)-C and Pd/$Fe_3O_4$(5%)-C catalysts showed a higher current density of the peak $r_p$, while Pd/$Fe_3O_4$(10%)-C catalyst showed a decline on the peak $r_p$ current density. The peak $r_p$ current density of methanol oxidation on the Pd/$Fe_3O_4$(5%)-C catalyst was over 1.7 times larger than that on the Pd/C. Also, the Pd/$Fe_3O_4$(5%)-C catalyst exhibited a highest current density for the anodic peak $r_n$ in the reverse scan. It is generally suggested that the reverse anodic peak $r_n$ can be attributed to the removal of the incompletely oxidized carbonaceous species produced by the methanol oxidation in the positive-going scan[20-22]. These carbonaceous species are adsorbed on the active sites of Pd-based catalyst, leading to the so-called poisoning effect of the catalyst. The peak current density ratio of $r_p$ to $r_n$ ($j(r_p)/j(r_n)$) can be used to roughly understand the anti-poisoning ability of the catalyst. Accord ing to Fig. 4A, the $j(r_p)/j(r_n)$ values on the Pd/$Fe_3O_4$(2%)-C, Pd/$Fe_3O_4$(5%)-C, Pd/$Fe_3O_4$(10%)-C and Pd/C catalysts were calculated to be 2.62, 2.24, 2.49 and 2.14, respectively, implying that the presence of $Fe_3O_4$ improved the anti-poisoning ability of the Pd/C.

Electroactivities of the prepared catalysts for ethanol oxidation followed the same order as those for methanol oxidation, as indicated in Fig. 4B. The Pd/$Fe_3O_4$(5%)-C catalyst also showed the highest current density in the positive-going scan. The peak $r_p$ current density of ethanol oxidation on the Pd/$Fe_3O_4$-(5%)-C catalyst exceeded 1.4 times larger than that on the Pd/C. The onset potential for ethanol oxidation on the Pd/$Fe_3O_4$(5%)-C catalyst was ca. 70 mV negatively shifted as compared to that on the Pd/C catalyst. The values of $j(r_p)/j(r_n)$ for ethanol oxidation (Fig. 4B) on the Pd/$Fe_3O_4$(2%)-C, Pd/$Fe_3O_4$(5%)-C, Pd/$Fe_3O_4$(10%)-C and Pd/C catalysts were 0.9, 1.2, 0.8 and 1.3, respectively. In addition, the current densities on the prepared catalysts for ethanol oxidation (Fig. 4A and Fig. 4B) were unexceptionally higher than those for methanol oxidation. These results might be related to the intermediates obtained during ethanol oxidation in the positive-going scan. For methanol oxidation on the Pd-based catalysts, the intermediates were linearly formed species, marked as Pd=C=O[23], while for ethanol oxidation, the formed intermediates were the adsorbed ethoxy Pd-$CH_3CO$[24]. Pd=C=O species would be more stable than Pd-$CH_3CO$, and the number of the active sites during methanol oxidation might decline more significantly than that during ethanol oxidation, resulting in the decrease of

methanol oxidation current density.

Electro-oxidations of *n*-propanol and iso-propanol on the catalysts are shown in Fig. 4C and Fig. 4D. It is clearly seen that the Pd/$Fe_3O_4$(5%)-C catalyst showed the highest current density on the positive-going scan for either *n*-propanol oxidation or iso-propanol oxidation. The Pd/$Fe_3O_4$(5%)-C catalyst displayed the peak $r_p$ current density of 180.5 mA·$cm^{-2}$ for *n*-propanol oxidation and 53.9 mA·$cm^{-2}$ for iso-propanol oxidation, which are over 1.7 and 1.3 times larger than the Pd/C, respectively. Additionally, for all of the prepared catalysts, the current densities on the forward scan for the *n*-propanol oxidation were always higher than those for other alcohols oxidations, and iso-propanol oxidation presented the lowest current density. According to different electro-oxidation mechanisms of the alcohols tested on Pd-based catalysts[7], the intermediates for *n*-propanol oxidation were the adsorbed species Pd-$CH_3CH_2CO$, which may be more likely to leave from the catalyst surface due to the longer carbon chain of Pd-$CH_3CH_2CO$ than those of Pd=C=O and Pd-$CH_3CO$. However, the electro-oxidation of iso-propanol on Pd-based catalysts went through a different mechanism, where the intermediates of iso-propanol oxidation could be represented by Pd-$CH_3CHOHCH_3$[7]. Formation of the Pd-$CH_3CHOHCH_3$ species might be relatively difficult than other intermediates, bringing about a lower current density of iso-propanol oxidation. This could be further corroborated from the CV profile of iso-propanol. It is found from Fig. 3 that for the oxidation of iso-propanol, the anodic current density after the anodic peak $r_p$ on the forward scan rapidly decreased to a lowest value corresponding to the anodic potential of ca.-0.05 V. However, for the oxidation of other alcohols (Figs. 4A, B and C), this anodic potential shifted to a more positive direction. In addition, an obvious cathodic peak at ca. -0.29 V on the reverse scan arised in the presence of iso-propanol (Fig. 4D), while this cathodic peak became weaker in the presence of other alcohols (Figs. 4A, B and C). Results revealed that in the presence of iso-propanol, the formation of Pd oxides on the Pd-based catalysts during the forward scan took place at a lower over-potential

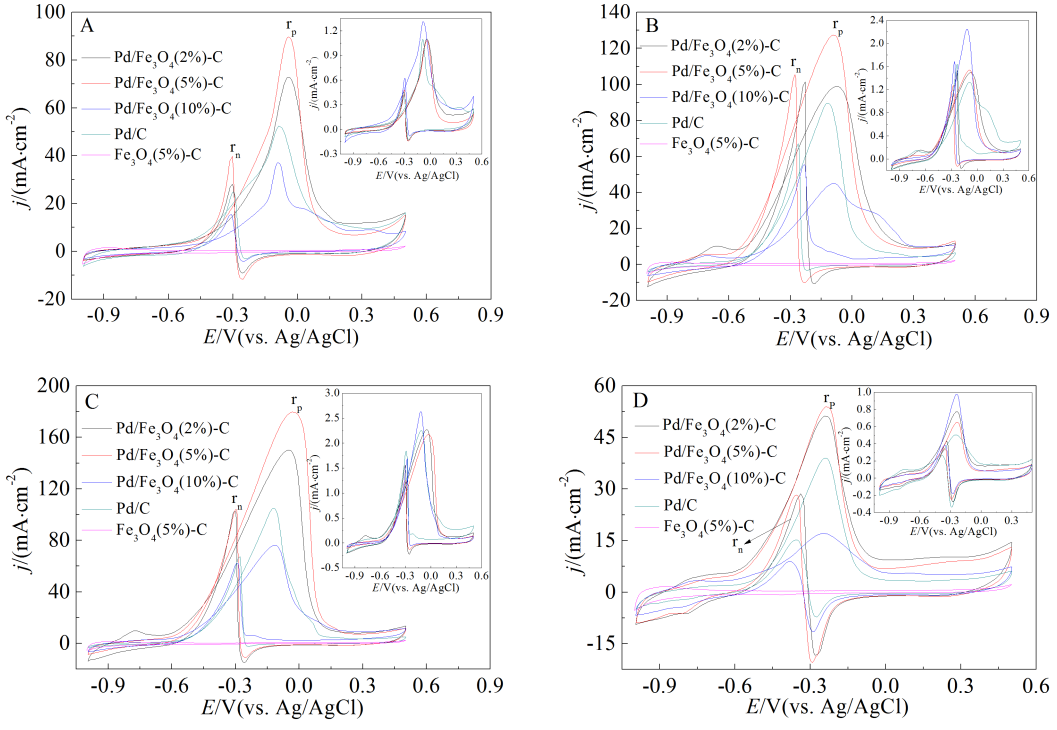


Fig. 4 Cyclic voltammograms of the prepared catalysts in 1 mol·$L^{-1}$ NaOH in the presence of 0.5 mol·$L^{-1}$ $CH_3OH$ (A), 0.5 mol·$L^{-1}$ $CH_3CH_2OH$ (B), 0.5 mol·$L^{-1}$ *n*-$CH_3CH_2CH_2OH$ (C) and 0.5 mol·$L^{-1}$ iso-$CH_3CH_2CH_2OH$ (D). Scan rate: 50 mV·$s^{-1}$. Insets are the corresponding CVs where current densities are normalized by $S_{active\ Pd}$.

than in the presence of other alcohols, suggesting that the formation of Pd oxides in the presence of iso-propanol is relatively easy compared to other alcohols. For these alcohols, therefore, the prepared Pd-based catalysts exhibited the highest electroactivity for *n*-propanol oxidation, followed by ethanol, methanol and iso-propanol oxidation. In addition, the electroactivities of the prepared catalysts for oxidation of the alcohols tested were subordinated to the following order: $Pd/Fe_3O_4$(5%)-C > $Pd/Fe_3O_4$(2%)-C > Pd/C > $Pd/Fe_3O_4$(10%)-C.

Insets in Fig. 4 exhibited the CVs through which the current densities were normalized by the Pd active surface area ($S_{\text{active Pd}}$). It is found from the insets that for the oxidation of the alcohols tested, all the catalysts presented close current densities (vs. $S_{\text{active Pd}}$). Results showed that the increment on the dispersion of Pd nanoparticles in the presence of $Fe_3O_4$ caused the increase of the current densities as indicated in Fig. 4.

Electroactivities of the prepared catalysts for oxidations of methanol, ethanol, *n*-propanol and iso-propanol in 1 mol·$L^{-1}$ NaOH solutions were further investigated with chronoamperometric (CA) technique, as indicated in Fig. 5. It is observed from Fig. 5 that all the catalysts presented the largest stable current density for *n*-propanol oxidation, followed by ethanol, methanol and iso-propanol oxidations, which is consistent with the results from CVs (Fig. 4). The high current densities at the initial step of electrolysis were suggestively due to the double layer charging between the interface of electrode/electrolyte. For the methanol oxidation shown in Fig. 5A, the stable current density at 1800 s on $Pd/Fe_3O_4$(5%)-C catalyst was over 1.8, 2.7 and 4.9 times larger than that on $Pd/Fe_3O_4$(2%)-C, $Pd/Fe_3O_4$(10%)-C and Pd/C catalysts, respectively, showing a larger stable current density difference between $Pd/Fe_3O_4$(5%)-C and other catalysts. However, the differences were reduced for the oxidations of ethanol (Fig. 5B), *n*-propanol (Fig. 5C) and iso-propanol (Fig. 5D), although the $Pd/Fe_3O_4$-(5%)-C catalyst still delivered the largest stable current density.

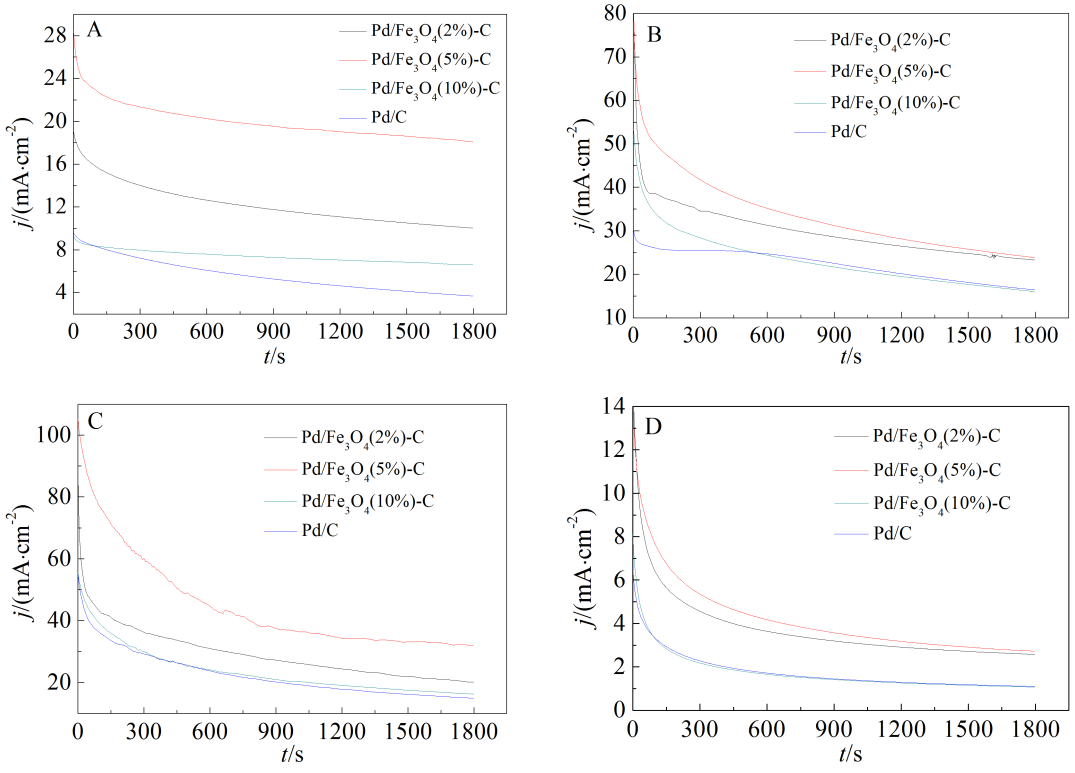


Fig. 5 Chronoamperometric responses of the prepared catalysts at -0.2 V in 1 mol·$L^{-1}$ NaOH in the presence of 0.5 mol·$L^{-1}$ $CH_3OH$ (A), 0.5 mol·$L^{-1}$ $CH_3CH_2OH$ (B), 0.5 mol·$L^{-1}$ *n*-$CH_3CH_2CH_2OH$ (C) and 0.5 mol·$L^{-1}$ iso-$CH_3CH_2CH_2OH$ (D).

Electrocatalytic stabilities of the $Pd/Fe_3O_4(5\%)$-C and Pd/C as two typical representatives of the prepared catalysts were also studied using repeatedly sweeping cyclic voltammetry. Fig. 6 shows 400 successive sweeping CV profiles of the two catalysts in 1 mol·$L^{-1}$ NaOH solutions in the presence of 0.5 mol·$L^{-1}$ ethanol. It is observed from Fig. 6 that the anode current density on the forward-going scan declined with the increasing in the number of successive cycle sweep. It can be found from CVs of $Pd/Fe_3O_4(5\%)$-C catalyst (Fig. 6A) that the anode peak ($r_p$) current density on the forward-going scan for the 100th cycle was 86% of that for the 1st cycle. All the same, the anode current density after the 100th cycle remained almost unchanged, showing that a relatively steady electro-oxidation of ethanol on the $Pd/Fe_3O_4(5\%)$-C was reached. Fig. 6A also shows that the $r_p$ current density for the 400th cycle was 66% of that for the 1st cycle and 95% of that for the 300th cycle. The decrease of the anode current density from the 1st to 100th cycle could be attributed to the consumption of ethanol near the interface of catalyst/solution. As for the Pd/C catalyst as indicated in Fig. 6B, the changing trend of the anode current density with the cycle sweeping number was similar to the $Pd/Fe_3O_4(5\%)$-C catalyst, except that on the Pd/C catalyst, the rp peak current density displayed a relatively rapid decline with the cycle sweeping number. The $r_p$ current density for the 400th cycle was 51% of that for the 1st cycle and 89% of that for the 300th cycle.

Electrochemical impedance spectroscopy (EIS) was also used to investigate the electroactivity of the prepared catalysts for ethanol oxidation. Fig. 7 shows Nyquist diagrams of the $Pd/Fe_3O_4(5\%)$-C and Pd/C catalysts at -0.2 V in 1 mol·$L^{-1}$ NaOH containing 0.5 mol·$L^{-1}$ ethanol. Both $Pd/Fe_3O_4(5\%)$-C and Pd/C catalysts presented a well-defined semicircle in the range of the frequency tested, which is caused by the electrocatalytic oxidation of ethanol. Compared to Pd/C catalyst, $Pd/Fe_3O_4(5\%)$-C catalyst exhibited a significant decrease of the semicircle diameter. This was attributed to the lowering of the charge transfer resistance for ethanol oxidation on the $Pd/Fe_3O_4(5\%)$-C catalyst. The inset in Fig. 7 presents the equivalent electric circuit used to fit the Nyquist diagrams, where $R1$ represents solution resistance and $R2$ represents charge transfer resistance involved in ethanol oxidation. It is found from Fig. 7 that the fitting curves (solid line) are well consistent with the experimental data (dots), indicating the reasonably good fitting with the equivalent circuit. Values of the corresponding equivalent circuit elements obtained by fitting the experimental data are listed in Table 1. A small change in $R1$ values for Pd/C and $Pd/Fe_3O_4(5\%)$-C catalysts would be ascribed to the error caused by the fitting process. The charge transfer resistance $R2$, involved in the electrochemical oxidation of ethanol, displayed a much lower value on the $Pd/Fe_3O_4(5\%)$-C catalyst than on the Pd/C catalyst. This shows that kinetic performance of ethanol oxidation on the $Pd/Fe_3O_4(5\%)$-C catalyst was well improved as compared to that on the Pd/C.

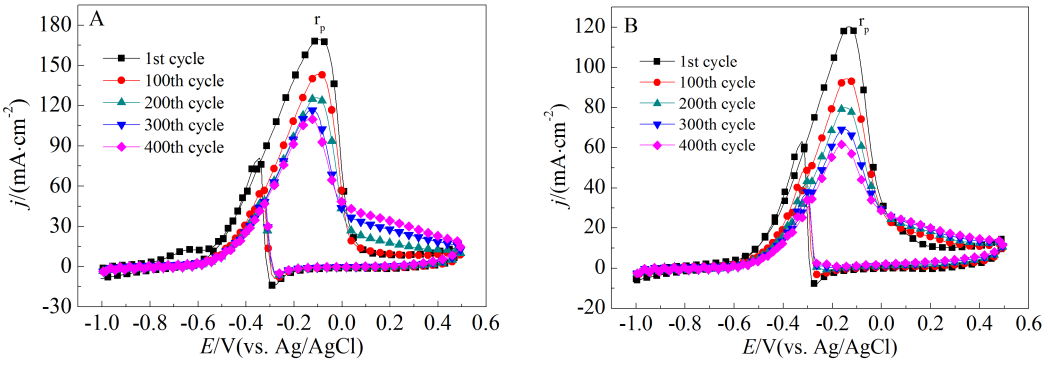


Fig. 6 400-continuous-cycle sweeps of the $Pd/Fe_3O_4(5\%)$-C (A) and Pd/C (B) catalysts in 1 mol·$L^{-1}$ NaOH containing 0.5 mol·$L^{-1}$ ethanol at a scan rate of 100 mV·$s^{-1}$

Tab. 1　Simulation data of impedance spectra from Fig. 7

| catalyst | *R*1/Ω | *R*2/Ω | *Q*1-Y0 | *Q*1-n | *Q*2-Y0 | *Q*2-n | *R*3/Ω | *C*1/kF |
|---|---|---|---|---|---|---|---|---|
| Pd/C | 16.86 | 204 | 4.58E-04 | 0.84204 | 0.6938 | 0.489 | -41.4 | 1 |
| Pd/$Fe_3O_4$(5%)-C | 12.47 | 53.84 | 6.46E-04 | 0.886 | 0.6938 | 0.489 | -41.4 | 1 |

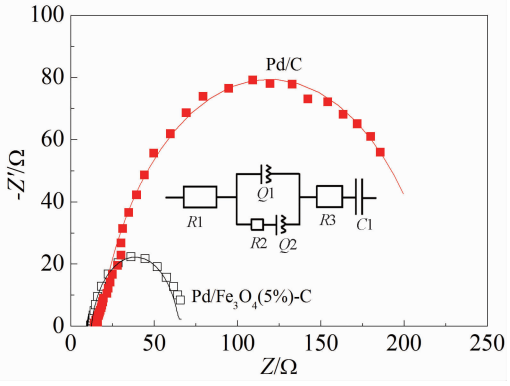


Fig. 7　Electrochemical impedance spectra (symbols) and the fitted curves (solid lines) of the Pd/$Fe_3O_4$(5%)-C and Pd/C catalysts in 1 mol·$L^{-1}$ NaOH containing 0.5 mol·$L^{-1}$ ethanol at a potential of -0.2 V. Amplitude of modulation potential was 10 mV. Frequency was changed from 10 kHz to 50 MHz. Inset shows the corresponding equivalent electric circuit compatible with the Nyquist diagrams, where *R*1: electrolyte solution resistance; *R*2: charge transfer resistance; *R*3: negative resistance effect of porous material; *Q*1 and *Q*2: constant phase element (CPE); C1: electrochemical capacitor.

As for the role of $Fe_3O_4$ played in the enhancement of Pd/C electroactivity, it would act as a co-catalyst for alcohol oxidation. According to the mechanism of alcohol oxidation on Pd-based catalysts[7], the following three steps are generally accepted to elucidate the alcohol electro-oxidation path: 1) adsorption of alcohol on Pd active sites to form the adsorbed intermediate; 2) formation of the adsorbed OH on Pd active sites ($OH_{ad}$); and 3) reaction between the adsorbed intermediate and $OH_{ad}$ to form the products. Clearly, the adsorption strength of $OH_{ad}$ on Pd active sites greatly influences the oxidation rate of alcohols. Presence of $Fe_3O_4$ weakens the adsorption strength of OH on the Pd active site, and hence, facilitates the reaction between $OH_{ad}$ and the adsorption intermediate. More Pd active sites will be produced with the reaction of $OH_{ad}$ and the adsorbed intermediate, which is conductive to the further formation of $OH_{ad}$. Therefore, the presence of proper amount of $Fe_3O_4$ can speed up the alcohol oxidation rate. On the other hand, $Fe_3O_4$ itself has no electroactivity for alcohol oxidation and thus excessive amounts of $Fe_3O_4$ will lead to a drop in the adsorbed $OH_{ad}$ concentration, which is unfavourable to the alcohol oxidation.

Finally, the results from the present study are compared with those of the alcohol oxidation reaction activities from several other Pd-based catalysts reported earlier in Table 2. The data show that the Pd/$Fe_3O_4$(5%)-C catalyst was superior to most of the previously reported Pd-based catalysts by considering both the on set potential and the current density at -0.1 V.

Tab. 2　Comparison of the present work with the reference results

| Catalyst | Onset potential/ V(vs. Ag/AgCl) | Current density/ (mA·$cm^{-2}$) | Electrolyte | Scan rate/ (mV·$s^{-1}$) | Ref. |
|---|---|---|---|---|---|
| PdPt/CNTs | -0.67 | 107 | 0.5 mol·$L^{-1}$ NaOH + 0.5 mol·$L^{-1}$ $C_2H_5OH$ | 50 | [4] |
| Ni@Pd/MWCNTs | -0.55 | 71.5 | 1 mol·$L^{-1}$ KOH + 1.0 mol·$L^{-1}$ $C_2H_5OH$ | 50 | [14] |
| Pd-NiO/C | -0.6 | 14.76 | 1 mol·$L^{-1}$ KOH + 0.5 mol·$L^{-1}$ $C_2H_5OH$ | 50 | [18] |
| PdRuSn/C | -0.74 | 62.5 | 0.5 mol·$L^{-1}$ NaOH + 3.0 mol·$L^{-1}$ $C_2H_5OH$ | 50 | [21] |
| Pd/Ti | -0.65 | 6.4 | 1.0 mol·$L^{-1}$ KOH + 1.0 mol·$L^{-1}$ $C_2H_5OH$ | 5 | [24] |
| Pd/$Fe_3O_4$(5%)-C | -0.65 | 127.6 | 1 mol·$L^{-1}$ NaOH + 0.5 mol·$L^{-1}$ $C_2H_5OH$ | 50 | This work |

## 3 Conclusions

In this work, the Pd-$Fe_3O_4$ composite catalysts were prepared by depositing Pd nanoparticles on $Fe_3O_4$/C. Their morphological structures were characterized by well-dispersed Pd nanoparticles on carbon particles. The Pd particles with sizes of 5 ~ 13 nm were well-dispersed on the $Fe_3O_4$/C support. The Pd/$Fe_3O_4$(5%)-C catalyst displayed the largest active Pd area among the prepared catalysts. Cyclic voltammetric and chronoamperometric responses of the catalysts showed that the Pd/$Fe_3O_4$(5%)-C catalyst presented the best electroactivities for oxidations of methanol, ethanol, *n*-propanol and iso-propanol. The anodic oxidation current density of *n*-propanol on all of the prepared catalysts was always larger than those of other alcohols (methanol, ethanol and iso-propanol). Compared to the Pd/C, the Pd/$Fe_3O_4$(5%)-C also exhibited a much lower charge transfer resistance for ethanol oxidation, showing that the kinetic performance of ethanol oxidation on the Pd/$Fe_3O_4$(5%)-C was greatly improved. In addition, the Pd/$Fe_3O_4$(5%)-C catalyst presented high electroactive stability for ethanol oxidation.

## References:


[1] García-Cruz L, Casado-Coterillo C, Irabien Á, et al. Performance assessment of polymer electrolyte membrane electrochemical reactor under alkaline conditions-a case study with the electrooxidation of alcohols[J]. Electrochimica Acta, 2016, 206: 165-173.

[2] Cai J D, Huang Y Y, Guo Y L. PdTex/C nanocatalysts with high catalytic activity for ethanol electro-oxidation in alkaline medium[J]. Applied Catalysis B: Environmental, 2014, 150-151(9): 230-237.

[3] Goel J, Basu S. Pt-Re-Sn as metal catalysts for electro-oxidation of ethanol in direct ethanol fuel cell[J]. Energy Procedia, 2012, 28: 66-77.

[4] Yang G, Zhou Y, Pan H B, et al. Ultrasonic-assisted synthesis of Pd-Pt/carbon nanotubes nanocomposites for enhanced electro-oxidation of ethanol and methanol in alkaline medium[J]. Ultrasonics Sonochemistry, 2016, 28: 192-198.

[5] Yi Q F, Zou T, Zhang Y Y, et al. A novel alcohol/iron(III) fuel cell[J]. Journal of Power Sources, 2016, 321: 219-225.

[6] Yi Q F, Chen Q H. In situ preparation and high electrocatalytic activity of binary Pd-Ni nanocatalysts with low Pd-loadings[J]. Electrochimica Acta, 2015, 182: 96-103.

[7] Yi Q F, Chu H, Chen Q H, et al. High performance Pd, PdNi, PdSn and PdSnNi nanocatalysts supported on carbon nanotubes for electrooxidation of $C_2C_4$ alcohols[J]. Electroanalysis, 2015, 27(2): 388-397.

[8] Yang H J, Wang H L, Ji S, et al. Synergy between isolated-$Fe_3O_4$ nanoparticles and $CN_x$ layers derived from lysine to improve the catalytic activity for oxygen reduction reaction[J]. International Journal of Hydrogen Energy, 2014, 39(8): 3739-3745.

[9] Huang Y, Liu Y, Yang Z, et al. Synthesis of yolk/shell $Fe_3O_4$-polydopamine-graphene-Pt nanocomposite with high electrocatalytic activity for fuel cells[J]. Journal of Power Sources, 2014, 246(3): 868-875.

[10] Hong C Y(洪春艳). Preparation and characterization of Au/$Fe_3O_4$ nanoparticles and Pt/Au/$Fe_3O_4$ catalysts[D]. Beijing University of Chemical Technology(北京化工大学), 2013: 59-68.

[11] Fu Z, Yan L, Li K, et al. The performance and mechanism of modified activated carbon air cathode by non-stoichiometric nano $Fe_3O_4$ in the microbial fuel cell[J]. Biosensors & Bioelectronics, 2015, 74: 989-995.

[12] Wang Y, Zhao Y, Yin J, et al. Synthesis and electrocatalytic alcohol oxidation performance of Pd-Co bimetallic nanoparticles supported on graphene[J]. International Journal of Hydrogen Energy, 2014, 39(3): 1325-1335.

[13] Zalineeva A, Serov A, Padilla M, et al. Nano-structured Pd-Sn catalysts for alcohol electro-oxidation in alkaline medium[J]. Electrochemistry Communications, 2015, 57: 48-51.

[14] Zhang M, Yan Z, Xie J. Core/shell Ni@Pd nanoparticles supported on MWCNTs at improved electrocatalytic performance for alcohol oxidation in alkaline media[J]. Electrochimica Acta, 2012, 77(9): 237-243.

[15] Yi Q F, Sun L Z, Liu X P, et al. Palladium-nickel nanoparticles loaded on multi-walled carbon nanotubes modified with $\beta$-cyclodextrin for electrooxidation of alcohols[J]. Fuel, 2013, 111: 88-95.

[16] Yi Q F, Niu F G, Song L H, et al. Electrochemical activity of novel titanium-supported porous binary Pd-Ru particles for ethanol oxidation in alkaline media[J]. Electroanalysis, 2011, 23(9): 2232-2240.

[17] Shen P K, Xu C. Alcohol oxidation on nanocrystalline oxide Pd/C promoted electrocatalysts[J]. Electrochemistry Communications, 2006, 8(1): 184-188.

[18] Hu F, Chen C, Wang Z, et al. Mechanistic study of ethanol oxidation on Pd-NiO/C electrocatalyst[J]. Electrochimica

Acta, 2006, 52(3): 1087-1091.

[19] Wang H L(王海丽). Studies on oxygen reduction reaction of Pt/C electro-catalyst modified by $Fe_3O_4$[D]. Dalian Jiaotong University(大连交通大学), 2010: 29.

[20] Manohara R, Goodenough J B. Methanol oxidation in acids on ordered NiTi[J]. Journal of Materials Chemistry, 1992, 2(8): 875-887.

[21] Modibedi R M, Masombuka T, Mathe M K. Carbon supported Pd-Sn and Pd-Ru-Sn nanocatalysts for ethanol electro-oxidation in alkaline medium[J]. International Journal of Hydrogen Energy, 2011, 36(8): 4664-4672.

[22] Liu Z, Guo B, Hong L, et al. Microwave heated polyol synthesis of carbon-supported PtSn nanoparticles for methanol electrooxidation[J]. Electrochemistry Communications, 2006, 8(1): 83-90.

[23] Liu Z, Zhang X, Hong L. Physical and electrochemical characterizations of nanostructured Pd/C and PdNi/C catalysts for methanol oxidation[J]. Electrochemistry Communications, 2009, 11(4): 925-928.

[24] Liu J, Ye J, Xu C, et al. Kinetics of ethanol electrooxidation at Pd electrodeposited on Ti[J]. Electrochemistry Communications, 2007, 9(9): 2334-2339.

# $Pd/Fe_3O_4$-C 催化剂对甲醇、乙醇和丙醇氧化的电催化活性

邹　涛[1]，易清风[1,2*]，张媛媛[1]，刘小平[1]，徐国荣[1]，聂会东[1]，周秀林[1]

(1. 湖南科技大学化学化工学院，湖南 湘潭 411201；2. 理论有机化学与功能分子教育部重点实验室，湖南 湘潭 411201)

**摘要：** 制备对醇氧化反应具有优异电活性的钯催化剂是醇燃料电池研究的重要内容. 本文用硼氢化钠还原法制备了钯纳米颗粒，然后沉积在 $Fe_3O_4$/C 复合物表面，得到了不同 $Fe_3O_4$ 负载量的 $Pd/Fe_3O_4$-C 催化剂. 透射电镜（TEM）检测显示，钯纳米颗粒均匀地分散在 $Fe_3O_4$/C 表面. 对制备好的 $Pd/Fe_3O_4$-C 催化剂进行了循环伏安法（CV）、计时电流（CA）和电化学阻抗谱（EIS）的测试，研究了其在碱性介质中对 C1-C3 醇类（甲醇、乙醇和丙醇）氧化的电催化活性. 结果表明，所制备的不同 $Fe_3O_4$ 负载量的 $Pd/Fe_3O_4$(2%)-C、$Pd/Fe_3O_4$(5%)-C、$Pd/Fe_3O_4$(10%)-C 和 Pd/C 催化剂中，$Pd/Fe_3O_4$(5%)-C 催化剂表现出最高的醇氧化电流密度. 依据循环伏安（CV）数据，$Pd/Fe_3O_4$(5%)-C 催化剂对甲醇、乙醇、正丙醇和异丙醇氧化的阳极峰电流密度分别是 Pd/C 催化剂的 1.7、1.4、1.7 和 1.3 倍. $Pd/Fe_3O_4$(5%)-C 催化剂对乙醇氧化的电荷传递电阻也远低于 Pd/C 催化剂. 制备的所有催化剂对 C1-C3 醇类电氧化的电流密度大小排序如下：正丙醇 > 乙醇 > 甲醇 > 异丙醇. 此外，碳粉中 $Fe_3O_4$ 纳米颗粒的存在提高了钯纳米颗粒的电化学稳定性.

**关键词：** 钯催化剂；$Fe_3O_4$；醇氧化；电催化